ACS OMEGA

Open Access

http://pubs.acs.org/journal/acsodf

Article

Exploring the Anti-inflammatory Potential of Novel Chrysin Derivatives through Cyclooxygenase-2 Inhibition

Yuna Lee, Eun Ji Gu, Ha-Yeon Song, Bo-Gyeong Yoo, Jung Eun Park, Jongho Jeon,* and Eui-Baek Byun*

Cite This: *ACS Omega* 2024, 9, 50491−50503

Read Online

ACCESS | Metrics & More | Article Recommendations | Supporting Information

ABSTRACT: Inducible cyclooxygenase-2 (COX-2) is a crucial enzyme involved in the processes of inflammation and carcinogenesis, primarily by catalyzing the production of prostaglandin E2 (PGE2), a significant mediator of inflammation. In this study, we designed and synthesized a series of novel chrysin derivatives to evaluate their anti-inflammatory potential through COX-2 inhibition using *in vitro* cultures of RAW264.7 macrophages and *in silico* molecular docking assays. Among the synthesized derivatives, compounds **1a** and **8** demonstrated significant inhibition of lipopolysaccharide (LPS)-stimulated proinflammatory cytokine production, including interleukin-6 and tumor necrosis factor-alpha, in RAW264.7 cells. Additionally, these derivatives effectively inhibited PGE2 secretion through COX-2 enzyme inhibition in LPS-stimulated RAW264.7 cells. Molecular docking simulation results revealed that **1a** and **8** possess high binding affinities for the COX-2 active site, indicating a strong potential for enzyme inhibition. Furthermore, druglikeness and ADMET predictions for these compounds indicated favorable pharmacokinetic properties, suggesting their suitability as drug candidates. Therefore, compounds **1a** and **8** hold promise as potential anti-inflammatory agents for further development.

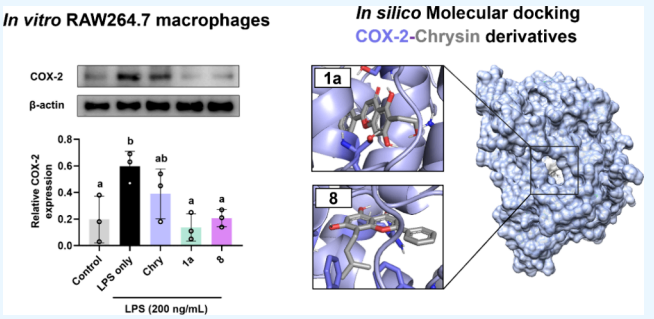

1. INTRODUCTION

Inflammation is the body's protective response activated by various stimuli, such as heat, radiation, and microbial invasion, and frequently results in tissue damage.[1] Cyclooxygenase-2 (COX-2; EC 1.14.99.1) is an inducible enzyme primarily activated during inflammatory processes, playing a critical role in the metabolism of arachidonic acid.[2] COX-2 catalyzes the conversion of arachidonic acid into prostaglandins, particularly prostaglandin E2 (PGE2), a key mediator of inflammation.[3] PGE2 triggers vascular hyperpermeability, pain sensation, and pyrexia,[4] and is implicated in the development and progression of various inflammatory disorders, including cancer,[5] arthritis,[6] and cardiovascular diseases.[7] Furthermore, the upregulation of COX-2 is closely associated with proinflammatory cytokines, such as interleukin-6 (IL-6) and tumor necrosis factor-alpha (TNF-α), which further amplify the inflammatory response.[8] Consequently, targeting COX-2 could be a promising strategy for the treatment of inflammation and its associated disorders. Various nonsteroidal anti-inflammatory drugs (NSAIDs) that inhibit COX-2, such as celecoxib and rofecoxib,[9] have been developed to mitigate inflammation; however, these agents are associated with adverse effects, including cardiovascular risks and gastrointestinal complications.[10,11] Moreover, several studies have indicated that certain NSAIDs, such as indomethacin and piroxicam, can trigger the production of cytokines like IL-6 and lead to hepatotoxicity.[12,13] These concerns underscore the importance of discovering and developing new COX-2 inhibitors that can provide effective anti-inflammatory benefits with reduced side effects.

Chrysin is a flavonoid primarily found in passionflower, honey, and propolis. Owing to its unique structural features, including two phenyl rings and a central three-carbon ring, chrysin exhibits strong antioxidant and anti-inflammatory properties, making it highly therapeutically potent.[14] For instance, Harris et al. (2006) demonstrated that chrysin inhibited COX-2−catalyzed PGE2 production in lipopolysaccharide (LPS)-stimulated murine RAW264.7 macrophages.[15] Additionally, chrysin was shown to suppress pro-inflammatory cytokines such as IL-6 and TNF-α in mast cells.[16] Rauf et al. (2015) further reported that chrysin interacted strongly with the COX-2 enzyme, consistent with an anti-inflammatory effect.[17] However, natural chrysin is limited in its therapeutic applications because of its low solubility and poor bioavailability

Received: August 29, 2024
Revised: October 28, 2024
Accepted: November 22, 2024
Published: December 10, 2024

Scheme 1. Synthesis of the Chrysin Derivative (5)

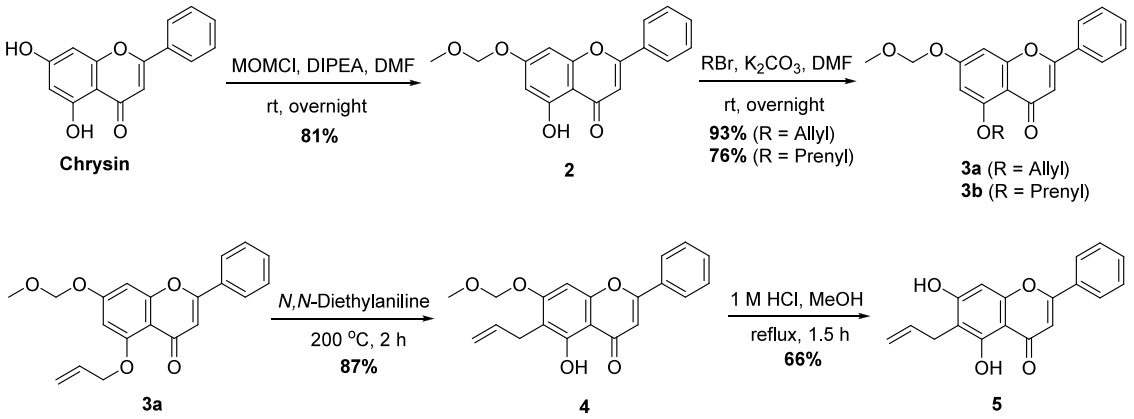

Scheme 2. Synthesis of the Chrysin Derivatives (8 and 10)

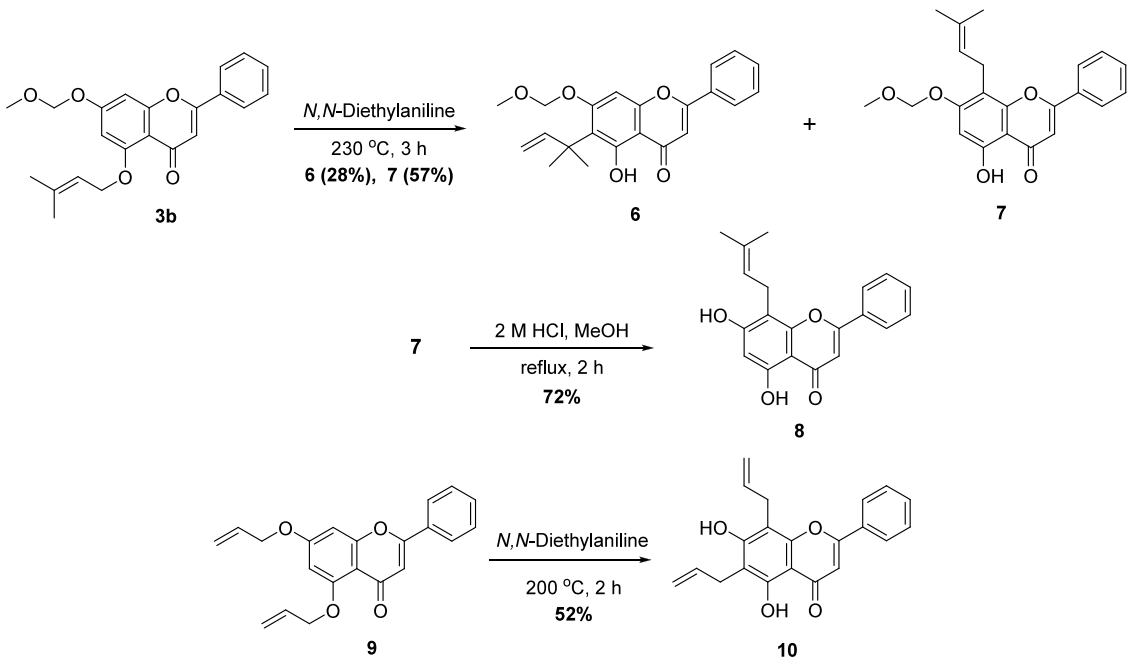

Scheme 3. Synthesis of Hydroxyethylated Chrysin (1a and 1b)

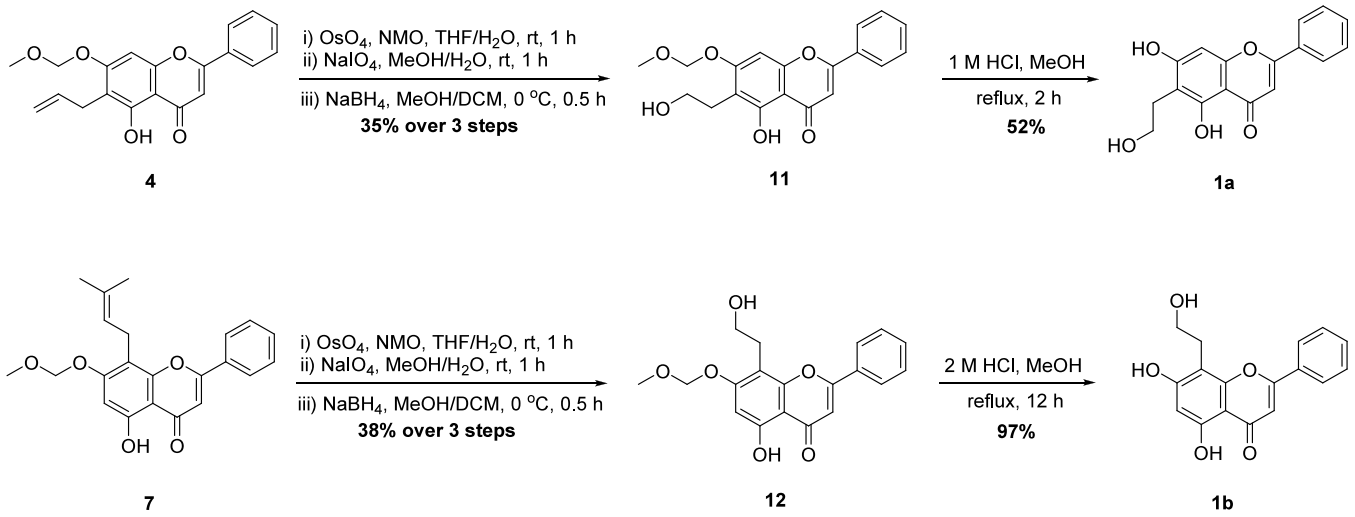

https://doi.org/10.1021/acsomega.4c07938
ACS Omega 2024, 9, 50491−50503

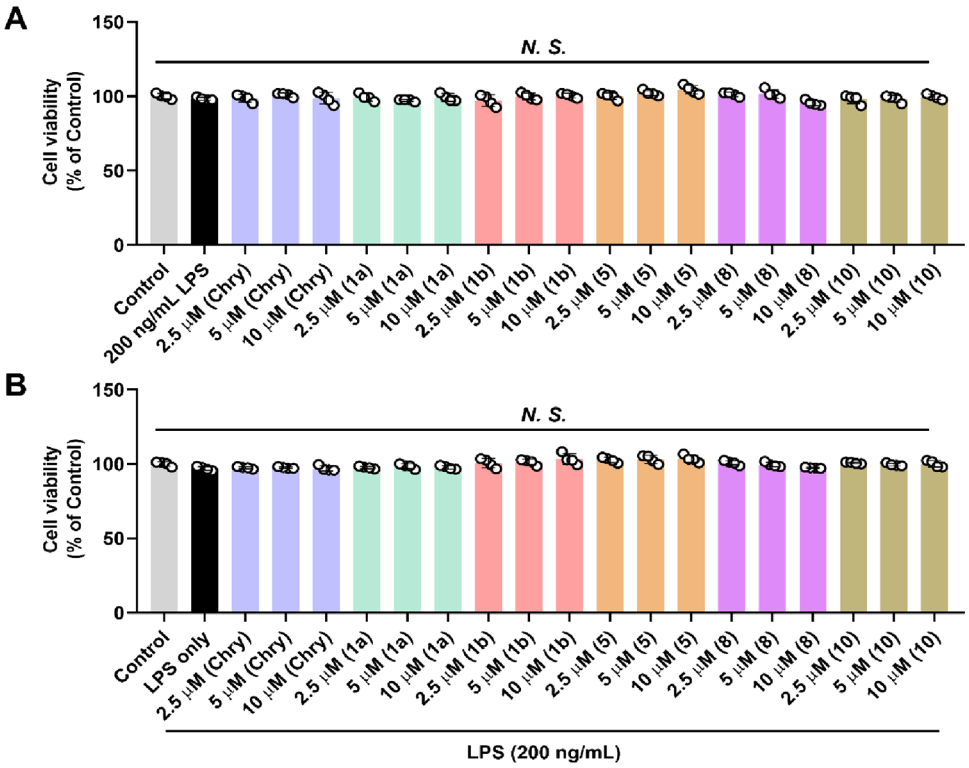

Figure 1. Evaluation of cell viability with synthetic chrysin derivatives. (A) Impact of chrysin derivatives on cell viability in RAW264.7 cells. Cells were exposed to varying concentrations (2.5, 5, and 10 μM) of chrysin or, compounds **1a**, **1b**, **5**, **8**, and **10** for 18 h, followed by the WST-1 assay. (B) Impact of chrysin derivatives on cell viability in LPS-stimulated RAW264.7 cells. Cells were treated with different concentrations (2.5, 5, and 10 μM) of chrysin or compounds 1a, 1b, 5, 8, and 10 in the presence of LPS (200 ng/mL) for 18 h. Data are presented as means ± SD ($n = 4$). Statistical differences were assessed using the Tukey-Kramer's test. *N.S.*, not significant at $p < 0.05$.

(less than 1%).[18] Therefore, medicinal applications of various chrysin derivatives produced through chemical synthesis or biotransformation have been explored.

Over the past few years, several chrysin derivatives with enhanced biological activities, including anti-inflammatory effects have been developed as potential drug candidates.[19−22] These new molecular structures, prepared using chrysin as the starting material, have been synthesized through various reactions such as alkylation, the Mannich reaction, addition−elimination, and sigmatropic rearrangement. In particular, we prepared a novel derivative with a hydroxyethyl group at the C8 position of chrysin using a radiation reaction. In previous studies, C8-hydroxyethyl chrysin has shown a stronger anti-inflammatory effect compared with that of unmodified chrysin, by inhibiting the expression of COX-2 and pro-inflammatory cytokines in LPS-stimulated macrophages.[23−26]

The production of C8-hydroxyethyl chrysin is achieved by gamma-irradiation of the starting material dissolved in a methanolic solution. This process offers the advantage of producing the desired product in fewer steps compared with conventional small-molecule synthesis. However, because of the high incidence of side reactions during the radiation process, it is not suitable for high-yield production. Consequently, purifying small quantities of C8-hydroxyethyl chrysin requires repeated preparative HPLC, making large-scale production highly inefficient. Establishing a reliable and efficient production method is essential for conducting the extensive *in vivo* experiments necessary to study clinical applications of such compounds. Additionally, radiation chemistry yields only a single outcome under specific conditions, resulting in lower research efficiency compared with that of conventional medicinal chemistry methods, which can simultaneously evaluate various derivatives and synthetic intermediates. To overcome these drawbacks, this study focused on the synthesis process of hydroxyethylated chrysin with an improved anti-inflammatory activity compared with that of chrysin.

2. RESULTS AND DISCUSSION

2.1. Chemistry. The synthetic procedures of the chrysin derivatives are illustrated in Schemes 1−3. The 7-hydroxy group of chrysin was protected selectively using methoxymethyl (MOM) chloride and *N*, *N*-diisopropylethylamine (DIPEA) at room temperature (Scheme 1).[27] Then, an allyl or prenyl group was introduced at the 5-hydroxy group of compound **2** to give rise to intermediate **3a** or **3b**, respectively. The Claisen rearrangement of **3a** was carried out at 200 °C using *N*,*N*-diethylaniline as the solvent, to produce chrysin 5-allyl ether (**4**) with an 87% yield. The MOM group in compound **4** was removed under acidic condition at an elevated temperature to give rise to compound **5**.

When the Claisen rearrangement of **3b**, containing a prenyl group, was conducted under slightly higher temperature (230 °C), it produced compound **6** with a quaternary carbon at the C6 position and compound **7** with the prenyl group migrated to the C8 position, with 28% and 57% yields, respectively (Scheme 2). The formation of product **7** appears to involve the initial migration of the prenyl group from **3b** to the C6 position, followed by a rearrangement of the C6 substituent to the C8 position. This reaction demonstrated that the product observed from the Claisen rearrangement is dependent on the substituent at the 5-hydroxy group of chrysin. When chrysin was reacted

https://doi.org/10.1021/acsomega.4c07938
ACS Omega 2024, 9, 50491−50503

with an excess of allyl bromide, 5,7-diallyl ether was formed (**9**). Interestingly, the Claisen rearrangement of **9** yielded product **10**, where allyl groups were rearranged to both the C6 and C8 positions. The MOM group in **7** was deprotected under acidic conditions, yielding **8**. The NMR spectra of compound **8** were consistent with the structural analysis reported in the previous literature.[28]

The allyl and prenyl substituents of chrysin derivatives **4** and **7** were readily converted into a hydroxyethyl group through three sequential steps: dihydroxylation of the alkene, oxidative cleavage of the diol, and reduction of the aldehyde (Scheme 3). Finally, the removal of the MOM group in compounds **11** and **12** under acidic conditions provided the desired products **1a** and **1b**, respectively.

2.2. Assessment of In Vitro Cell Viability Using the WST-1 Assay. To identify the optimal concentration for eliciting an inflammatory response, we assessed the cytotoxicity of synthetic chrysin derivatives (compounds **1a**, **1b**, **5**, **8**, and **10**) in the presence or absence of LPS (200 ng/mL) using the WST-1 assay. As shown in Figure 1A, none of the tested compounds exhibited significant cytotoxic effects in RAW264.7 cells at concentrations of 2.5, 5, and 10 μM when added for 18 h. Furthermore, the presence of LPS (200 ng/mL) did not impact cell viability under the experimental conditions (Figure 1B). Based on these results, the above concentrations were selected for subsequent assessments of their anti-inflammatory potential.

2.3. Preliminary Screening of Chrysin Derivatives for IL-6 Secretion Inhibition. IL-6 is a crucial cytokine in the immune reaction, produced by macrophages in response to infections and tissue injuries.[29] Elevated IL-6 levels are associated with chronic inflammatory conditions, making it a key target for anti-inflammatory therapy. In the present study, the synthesized chrysin derivatives were assessed for their potential to suppress IL-6 production in LPS-stimulated RAW264.7 cells. Among the tested compounds, **1a** and **8** at a concentration of 5 μM significantly reduced IL-6 levels ($p < 0.05$) compared with those in the LPS-only group, demonstrating a marked anti-inflammatory potential in murine macrophages (Figure 2). However, compounds **5** and **10** did not show a notable IL-6 inhibitory effect. Additionally, conventional NSAIDs, including indomethacin and piroxicam, tested at a concentration of 12.5 μM, did not significantly reduce LPS-induced IL-6 production (Figure S15). These findings suggest that while the anti-inflammatory effects of these NSAIDs may be limited in modulating cytokine production, particularly IL-6, the chrysin derivatives, particularly compounds **1a** and **8** could offer a promising alternative for suppressing cytokine production. Consequently, compounds **1a** and **8**, which exhibited effective IL-6 suppression, were chosen for further assessment of their anti-inflammatory activity.

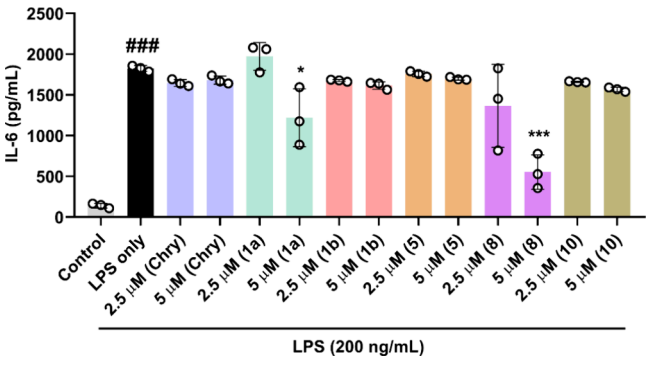

Figure 2. Inhibitory effects of synthetic chrysin derivatives on LPS-stimulated IL-6 secretion in RAW264.7 cells. Cells were incubated with chrysin or compounds **1a**, **1b**, **5**, **8**, and **10** (2.5 and 5 μM) in the presence of LPS (200 ng/mL). After 18 h incubation, the IL-6 level was determined using the CBA ELISA kit. Data are presented as means ± SD ($n = 3$). Statistical differences were assessed using the Tukey-Kramer's test; ###, $p < 0.001$ vs control; *, $p < 0.05$ vs LPS-only group; ***, $p < 0.001$ vs LPS-only group.

2.4. Dose-Dependent Effects of 1a and 8 on LPS-Stimulated IL-6 and TNF-α Secretion. Similarly to IL-6, TNF-α is a key mediator of inflammatory responses and is commonly elevated in various inflammatory and autoimmune diseases.[30] To further investigate the inhibitory activity of the potential candidates, **1a** and **8**, we evaluated their effects on LPS-induced IL-6 and TNF-α secretion at different doses (1.25, 2.5, 5, and 10 μM). At concentrations of 5 and 10 μM, compounds **1a** and **8** significantly ($p < 0.01$) reduced IL-6 levels compared to the LPS-only group (Figure 3A). Similarly, compound **8** demonstrated a dose-dependent inhibition ($p < 0.01$) of TNF-α levels at concentrations of ≥2.5 μM (Figure 3B). Taken together, both derivatives exhibited significant inhibitory effects compared to the LPS-only group, indicating their potential anti-inflammatory properties.

2.5. Inhibitory Effects of 1a and 8 on LPS-Stimulated PGE2 and COX-2 Protein Levels. COX-2 is a critical inflammatory mediator responsible for catalyzing the synthesis of PGE2.[31] Regulating COX-2 is essential for maintaining inflammatory homeostasis, making it a key molecular target for the prevention and treatment of inflammatory diseases. We first assessed the effect of various concentrations (1.25, 2.5, 5, and 10 μM) of compounds **1a** and **8** on the production of PGE2 in RAW264.7 cells stimulated with LPS. Treatment with compounds **1a** and **8** resulted in a dose-dependent inhibition of PGE2 production compared with that in the LPS-only group, with statistically significant reductions ($p < 0.05$) observed at concentrations of ≥10 μM and ≥5 μM, respectively (Figure 4A). Further, we evaluated the expression of COX-2 protein using Western blotting analysis. As depicted in Figure 4B and Figure S16, the LPS-only group exhibited a significant upregulation of COX-2 expression compared with that in the control group. However, treatment with compounds **1a** and **8** markedly attenuated ($p < 0.05$) this upregulation. This indicates that compounds **1a** and **8** may exert their anti-inflammatory effects by interfering with the COX-2 pathway, thereby reducing the production of inflammatory mediators. COX-2 expression is known to be regulated by key inflammatory signaling pathways, such as nuclear factor kappa-light-chain-enhancer of activated B cells and activator protein-1, which are activated in response to inflammatory stimuli like LPS. Although further investigations are needed, these pathways that contribute to COX-2 regulation may also be partially involved in the regulation of COX-2 expression by chrysin derivatives. Interestingly, the inhibitory effects of compounds **1a** and **8** on PGE2 production and COX-2 expression were more pronounced than those of the parent compound, chrysin. This suggests that these novel derivatives may possess superior anti-inflammatory efficacy.

To further quantify the inhibitory effects of chrysin, compounds **1a**, and **8** on COX-2 enzyme activity, we performed an *in vitro* COX-2 inhibition assay, which is based on the fluorometric detection of prostaglandin G2, the intermediate product generated by the COX-2 enzyme. The IC_{50} values for chrysin, compounds **1a**, and **8** were determined to be 18.48 μM,

https://doi.org/10.1021/acsomega.4c07938
ACS Omega 2024, 9, 50491−50503

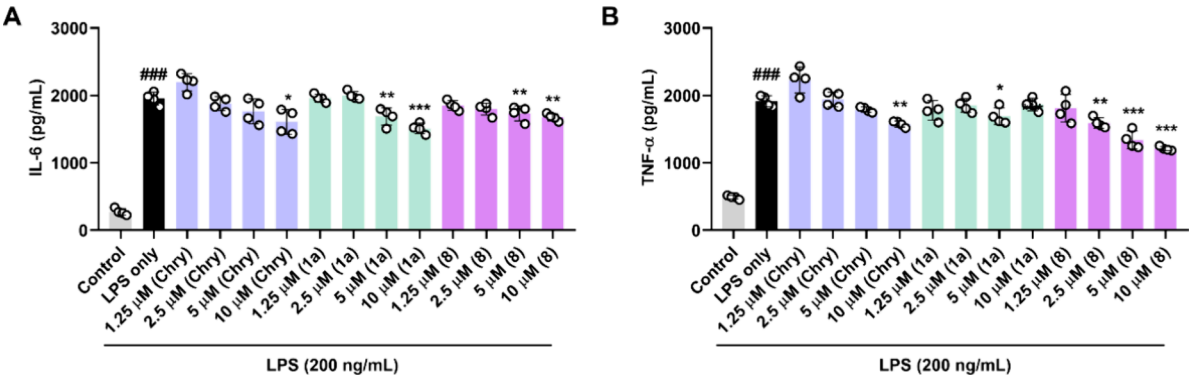

Figure 3. Inhibitory effects of compounds **1a** and **8** on LPS-stimulated cytokine secretion in RAW264.7 cells. Cells were treated with different concentrations of chrysin or compounds **1a** and **8** (1.25, 2.5, 5, and 10 μM) in the presence of LPS (200 ng/mL). Following 18 h incubation, IL-6 (A) and TNF-α (B) production was determined using the CBA ELISA kits. Data are presented as means ± SD (n = 4). Statistical differences were assessed using the Tukey-Kramer's test; ###, $p < 0.001$ vs control; *, $p < 0.05$ vs LPS-only group; **, $p < 0.05$ vs LPS-only group; ***, $p < 0.001$ vs LPS-only group.

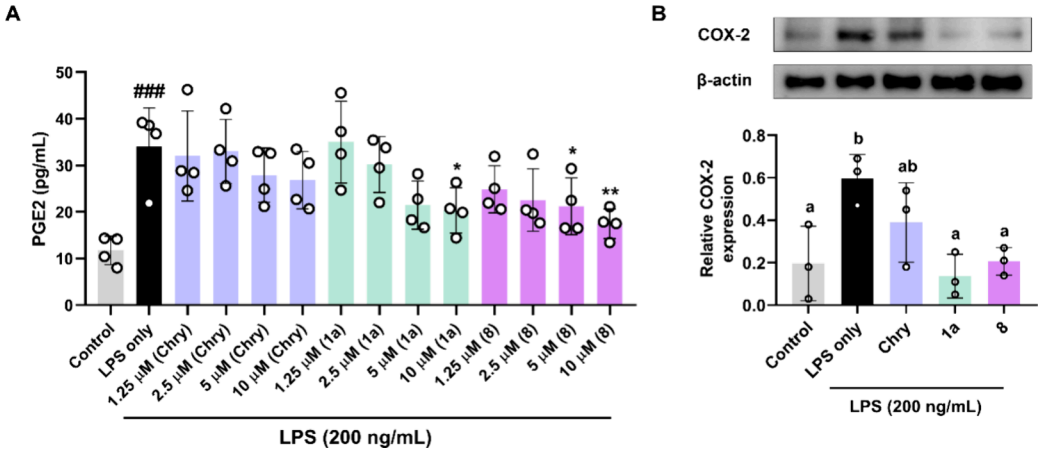

Figure 4. Inhibitory effects of compounds 1a and 8 on LPS-stimulated PGE2 and COX-2 in RAW264 cells. (A) Cells were treated with various concentrations of **1b** and **8** (1.25, 2.5, 5, and 10 μM) in the presence of LPS (200 ng/mL). After 18 h incubation, the PGE2 level was determined using the CBA ELISA kit. Data are presented as means ± SD (n = 4). Statistical differences were assessed using the Tukey-Kramer's test; ###, $p < 0.001$ vs control; *, $p < 0.05$ vs LPS-only group; **, $p < 0.05$ vs LPS-only group. (B) Cells were treated with chrysin or compounds **1a** and **8** (10 μM) for 18 h in the presence of LPS (200 ng/mL). COX-2 expression was quantified by Western blotting analysis. Data are presented as means ± SD (n = 3). Statistical differences were assessed using the Tukey-Kramer's test. Different letters on the columns indicate statistical differences at $p < 0.05$.

9.63 μM, and 6.76 μM, respectively (Table 1 and Figure S17). It is estimated that chrysin primarily enters cells via passive diffusion due to its lipophilic nature,[18] a mechanism likely shared by derivatives **1a** and **8** given their similar structures. Therefore, these derivatives are expected to use passive diffusion to reach intracellular targets like COX-2 and exert anti-inflammatory effects.

Table 1. Inhibitory Effects of Compounds 1a and 8 COX-2 Enzyme

compounds	IC_{50} (μM)
chrysin	18.48
compound **1a**	9.63
compound **8**	6.76

2.6. Molecular Modeling Study of COX-2 Interactions with Compounds 1a and 8. To further elucidate the interaction mechanisms of compounds **1a** and **8** with the COX-2 enzyme, a computational molecular docking study was conducted. The binding free energies (ΔG_{bind}), RMSD values, and specific binding interactions of indomethacin, chrysin, compounds **1a**, and **8** with COX-2 are summarized in Table 2

Table 2. Binding Free Energies (ΔG_{bind}), Root Mean Square Deviation (RMSD), Hydrogen Bonds, and Hydrophobic Interactions of Indomethacin, Chrysin, and Compounds 1a and 8 against the Active Site of the COX-2 Enzyme

ligands	binding energy (G_{bind}, kcal/mol)	RMSD (Å)	hydrogen bonds	hydrophobic interactions
indomethacin	−8.58	0.84	Arg120	Leu352, Val349, Leu384, Met522, Val523, Ala527, Leu531, Leu534
chrysin	−8.17	1.40	Arg120, Val349, Ser353	Val349, Tyr385, Trp387, Met522, Val523, Ala527
compound **1a**	−7.88	0.38	Arg120, Ser353, Ser530	Arg120, Val349, Tyr385, Trp387, Phe518, Met522, Val523, Ala527
compound **8**	−9.12	0.49	Arg120, Ser530	V349, Trp387, Phe518, Met522, Val523, Ala527

https://doi.org/10.1021/acsomega.4c07938
ACS Omega 2024, 9, 50491−50503

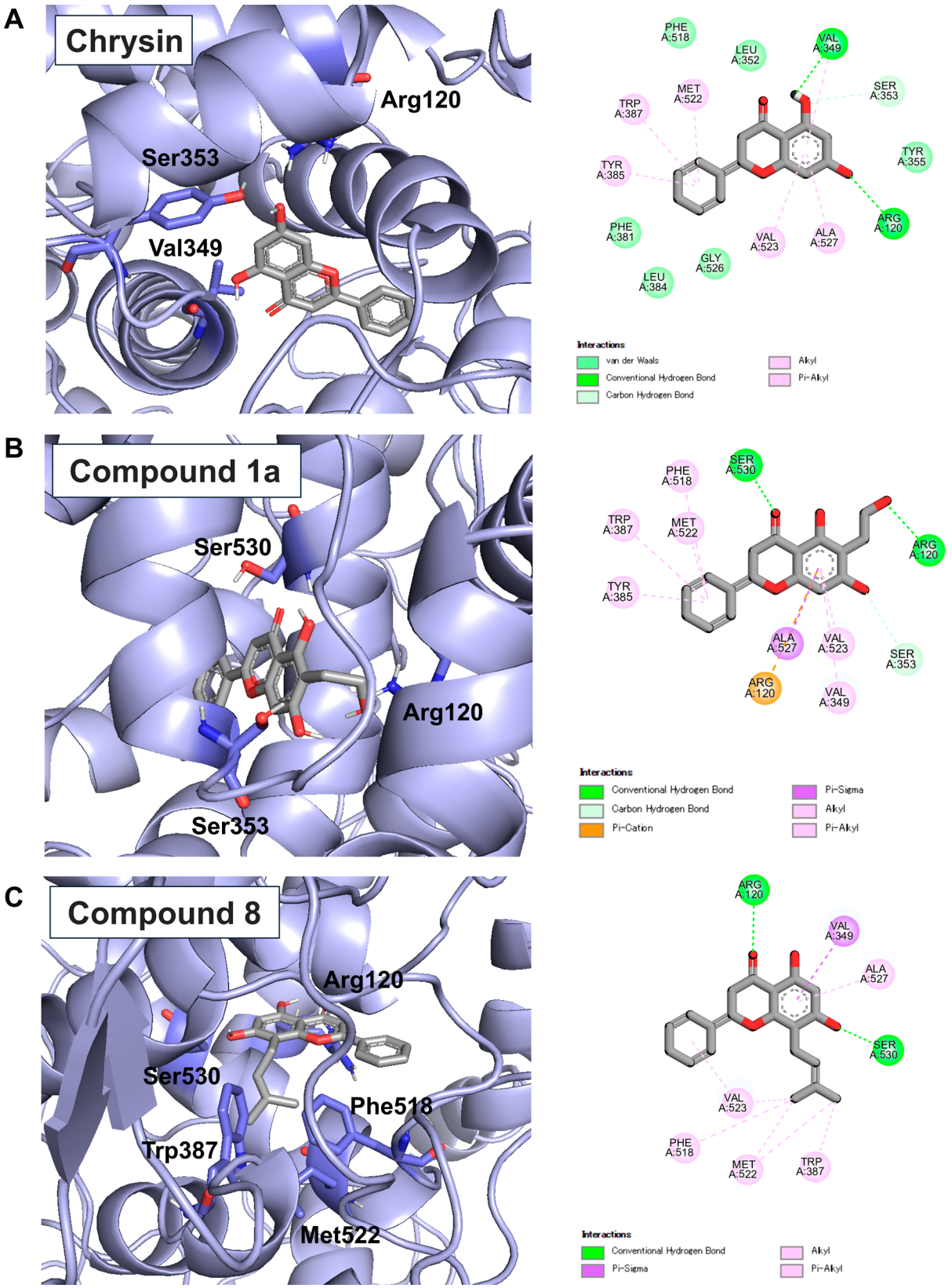

Figure 5. *In silico* molecular docking poses of (A) chrysin, (B) compound **1a**, and (C) compound **8** at the active site of the mouse COX-2 enzyme. The 3D interactions (left side) between the docked ligands and the active site of COX-2 were illustrated using PyMOL. The 2D views (right side) of the docking result were visualized using Discovery Studio.

and illustrated in Figure 5 and Figure S19. The RMSD values for each compound were all below 2 Å, thereby supporting the reliability and accuracy of the present docking results. According to several studies, binding affinities are generally considered strong when the ΔG_{bind} is less than −5.0 kcal/mol, and extremely strong when below −7.0 kcal/mol.[32,33] Indomethacin,

https://doi.org/10.1021/acsomega.4c07938
ACS Omega 2024, 9, 50491−50503

a well-known COX-2 inhibitor, exhibited a strong binding affinity (−8.58 kcal/mol) for the active site of COX-2, further demonstrating the reliability of our docking system in analyzing binding interactions (Figure S19).

Chrysin demonstrated a high binding affinity (−8.17 kcal/mol) within the COX-2 binding pocket, forming hydrogen bonds with Arg120, Val349, and Ser353 (Figure 5A). Additionally, chrysin exhibited five hydrophobic interactions, including alkyl and pi-alkyl types, with residues Tyr385, Trp387, Met522, Val523, and Ala527. These interactions underscore the potent inhibitory effect of chrysin on COX-2 enzymatic activity, consistent with previous studies on its anti-inflammatory activity.[17,34]

The ΔG_{bind} of compound 1a with the COX-2 enzyme was estimated to be −7.88 kcal/mol, indicating a slightly weaker but still significant binding affinity compared with that of chrysin. Within the COX-2 active site, compound **1a** formed hydrogen bonds with Arg120, Ser353, and Ser530, along with eight hydrophobic interactions involving Arg120, Val349, Tyr385, Trp387, Phe518, Met522, Val523, and Ala527 (Figure 5B). These interactions suggest a stable binding conformation, indicating a potential of compound **1a** for effective COX-2 inhibition.

Compound **8** demonstrated the strongest binding affinity, with a ΔG_{bind} of −9.12 kcal/mol, indicating robust interaction with the COX-2 binding pocket. Similarly to compound **1a**, compound **8** formed hydrogen bonds with Arg120 and Ser530 (Figure 5C). Additionally, it established eight hydrophobic interactions with Val349, Trp387, Phe518, Met522, Val523, and Ala527, five of which involved the prenyl group. Several studies have shown that prenylation in flavonoids increases lipophilicity of the molecule, thereby enhancing its affinity for biological membranes and interaction with cellular targets.[35−37] This modification can lead to improved biological activities, such as anti-inflammatory effects. Consequently, compound **8**'s stronger inhibitory effect on COX-2 compared to chrysin may be attributed to the introduction of a prenyl group at position 8 of the A ring.

Notably, Arg120 was a common amino acid residue interacting with indomethacin, chrysin, compounds **1a**, and **8**, highlighting its crucial role in COX-2 inhibition. Gundogdu-Hizliates et al. (2014) reported that Arg120, Tyr385, and Ser530 in COX-2 are key residues relevant to its enzymatic activity, particularly Arg120, which plays a crucial role in COX-2 inhibition.[38] Similarly, Yu et al. (2016) reported that Arg120 and Tyr385 are critical interacting residues for COX-2 inhibition.[39] Moreover, the interaction with Ser530 and Phe518, which was absent in chrysin but present in both derivatives, suggests that these residues likely contribute to the enhanced bioactivity of compounds **1a** and **8**. These findings emphasize that significance of hydrogen bonds and hydrophobic interactions in the inhibitory activity of compounds **1a** and **8** against the COX-2 enzyme.

2.7. In Silico Prediction of Pharmacokinetic Properties. The prediction of druglikeness properties and ADMET profiles indicated that both compounds **1a** and **8** could be promising candidates for drug development (Table 3). Both compounds complied with Lipinski's rule, showing no violations. Their parameters fell within the standard acceptable ranges: molecular weight <500 Da, logP ≤5, number of hydrogen bond acceptors ≤10, number of hydrogen donors ≤5, and number of rotatable bonds ≤10, and molar refractivity between 40 and 130. The predicted ADMET profiles were favorable: both compounds exhibited high human intestinal absorption rates, were not P-glycoprotein inhibitors, and did not inhibit CYP450 2D6, indicating a low risk of causing drug−drug interactions through these specific pathways. Additionally, both were predicted to be nonmutagenic and noncarcinogenic. These results suggest that compounds **1a** and **8** possess desirable pharmacokinetic properties and could serve as effective COX-2 inhibitors with potential anti-inflammatory effects for further development.

Table 3. Druglikeness Properties and *In Silico* ADMET Predictions of Chrysin, Indomethacin, and Compounds 1a and 8

	chrysin	indomethacin	1a	8
druglikeness properties				
Lipinski's rule	yes: 0 violation	yes: 0 violation	yes: 0 violation	yes: 0 violation
molecular weight (g/mol)	254.24	357.79	298.29	322.35
LogP	2.55	3.63	2.40	3.96
H-bond acceptors	4	4	5	4
H-bond donors	2	1	3	2
rotational bonds	1	5	3	3
molar refractivity	71.97	96.12	82.90	95.69
TPSA (Å^2)	70.67	68.53	90.90	70.67
ADMET properties				
human intestinal absorption (%)	98.87	95.09	97.80	99.59
P-glycoprotein inhibitor	no	no	no	no
CYP450 2D6 inhibitor	yes	no	no	no
mutagenicity	no	no	no	no
carcinogenicity	no	yes	no	no

3. CONCLUSIONS

The synthesized chrysin derivatives, particularly compounds **1a** and **8**, exhibited remarkable anti-inflammatory properties compared with those of the parent compound, chrysin. These derivatives significantly inhibited LPS-stimulated production of IL-6, TNF-α, and PGE2 via COX-2 inhibition in RAW264.7 cells. These inhibitory effects suggest strong potential of the derivatives as anti-inflammatory agents. Molecular docking studies further supported these findings, revealing that compounds **1a** and **8** have high binding affinities for the COX-2 active site, particularly interacting with crucial amino acid residues such as Arg120. These interactions were consistent with the observed *in vitro* anti-inflammatory activities, reinforcing the potential of the compounds as effective COX-2 inhibitors. Moreover, the druglikeness and ADMET predictions indicated favorable pharmacokinetic properties for compounds **1a** and **8**, underscoring their promise as viable drug candidates. However, to validate these findings, comprehensive *in vivo* studies are essential to evaluate the long-term safety and efficacy of these compounds. Therefore, compounds **1a** and **8** hold significant promise for development as novel anti-inflammatory agents, meriting further investigation in *in vivo* studies.

4. EXPERIMENTAL DETAILS

4.1. Chemicals. All reagents used are of analytical grade without further purification. Chrysin, chloromethyl methyl ether, allyl bromide, 3,3-dimethylallyl bromide, osmium tetroxide, 4-methylmorpholine *N*-oxide, and sodium (meta)-

https://doi.org/10.1021/acsomega.4c07938
ACS Omega 2024, 9, 50491−50503

periodate were purchased from Sigma-Aldrich Korea (Seoul, Korea). *N,N*-Dimethylaniline was purchased from TCI (Tokyo Chemical Industry Co., Tokyo, Japan). DIPEA was purchased from Daejung Chemicals & Metals Co. (Busan, Korea). Sodium borohydride was purchased from Samchun Chemical Co. (Seoul, Korea). MPLC (Medium Pressure Liquid Chromatography) purification of the product was carried out using a Biotage Selekt (Seongnam-si, Korea). ^{1}H NMR and ^{13}C NMR spectra were measured on a Bruker (AVANCE III 500 or 700 MHz) spectrometer and chemical shifts reported in ppm (d). Coupling constants (J) are reported in Hz. For each measurement, 0.75 mL of NMR solvent ($CDCl_3$ or DMSO-d_6) was used, with the temperature maintained at 25 °C. The ^{1}H NMR and ^{13}C NMR spectra were acquired with 16 and 2048 scans, respectively, using relaxation delay times of 1 s for ^{1}H NMR and 2 s for ^{13}C NMR. Mass spectral data were obtained using a JMS-700 high-resolution mass spectrometer (JEOL, Japan).

4.2. Synthesis of Compound 2. Chrysin (1.0 g, 3.93 mmol) was suspended in dry *N,N*-dimethylformamide (DMF) (20 mL) and DIPEA (1.38 mL, 7.86 mmol, 2 equiv) was added to the mixture. Then, chloromethyl methyl ether (0.6 mL, 7.86 mmol, 2 equiv) was added dropwise to the mixture. The reaction mixture was stirred at room temperature for 12 h. After the reaction was completed, the resulting mixture was extracted with ethyl acetate (EtOAc) (100 mL × 2) and saturated aqueous NH_4Cl solution (100 mL). The organic layer was dried over $MgSO_4$, filtered, and concentrated under reduced pressure. The crude product was purified by MPLC (EtOAc/Hexane) to give compound **2** (948 mg, 81%).

4.2.1. 5-Hydroxy-7-(methoxymethoxy)-2-phenyl-4H-chromen-4-one (2). ^{1}H NMR (700 MHz, $CDCl_3$): δ 12.67 (s, 1H), 7.90−7.89 (m, 2H), 7.56−7.51 (m, 3H), 6.68 (d, J = 2.21 Hz, 1H), 6.68 (s, 1H), 6.49 (d, J = 2.09 Hz, 1H), 5.25 (s, 2H), 3.51 (s, 3H). ^{13}C NMR (175 MHz, $CDCl_3$): δ 182.7, 164.2, 163.2, 162.2, 157.8, 132.0, 131.4, 129.2, 126.4, 106.5, 106.0, 100.3, 94.5, 94.4, 56.5. HR-MS (EI): calcd for $C_{17}H_{14}O_5$ $[M]^+$ 298.0841; found, 298.0843.

4.3. Synthesis of Compound 3a. To a solution of compound **2** (413 mg, 1.38 mmol) in DMF (20 mL), was added K_2CO_3 (691 mg, 5 mmol, 3.6 equiv). Then, allyl bromide (270 μL, 3 mmol, 2.2 equiv) was added dropwise to the mixture. The reaction mixture was then stirred at room temperature for 12 h. After the reaction was completed, the resulting mixture was extracted with EtOAc (100 mL × 2) and deionized water (100 mL). The organic layer was dried over $MgSO_4$, filtered, and concentrated under reduced pressure. The crude product was purified by MPLC (EtOAc/Hexane) to give compound **3a** (524 mg, 93%).

4.3.1. 5-(Allyloxy)-7-(methoxymethoxy)-2-phenyl-4H-chromen-4-one (3a). ^{1}H NMR (700 MHz, $CDCl_3$): δ 7.87−7.85 (m, 2H), 7.50−7.47 (m, 3H), 6.78 (d, J = 2.03 Hz, 1H), 6.65 (s, 1H), 6.47 (d, J = 2.22 Hz, 1H), 6.14−6.09 (m, 1H), 5.68 (dq, J = 10.7, 1.65 Hz, 1H), 5.35 (dq, J = 10.7, 1.37 Hz, 1H), 5.35 (s, 2H), 4.69−4.68 (m, 2H), 3.52 (s, 3H). ^{13}C NMR (175 MHz, $CDCl_3$): δ 177.4, 161.5, 160.8, 159.9, 159.6, 132.3, 131.6, 131.2, 129.0, 126.0, 117.9, 110.3, 109.0, 98.6, 96.0, 94.5, 69.9, 56.5. HR-MS (EI): calcd for $C_{20}H_{18}O_5$ $[M]^+$ 338.1154; found, 338.1157.

4.4. Synthesis of Compound 3b. To a solution of compound **2** (400 mg, 1.34 mmol) in DMF (20 mL) was added K_2CO_3 (278 mg, 2 mmol, 3.6 equiv). Then, 3,3-dimethylallyl bromide (464 μL, 4 mmol, 3 equiv) was added dropwise to the mixture. The reaction mixture was then stirred at room temperature for 12 h. After the reaction was completed, the resulting mixture was extracted with EtOAc (100 mL × 2) and deionized water (100 mL). The organic layer was dried over $MgSO_4$, filtered, and concentrated under reduced pressure. The crude product was purified by MPLC (EtOAc/Hexane) to give compound **3b** (371 mg, 76%).

4.4.1. 7-(Methoxymethoxy)-5-((3-methylbut-2-en-1-yl)oxy)-2-phenyl-4H-chromen-4-one (3b). ^{1}H NMR (700 MHz, $CDCl_3$): δ 7.84−7.82 (m, 2H), 7.46−7.44 (m, 3H), 6.73 (d, J = 2.24 Hz, 1H), 6.61 (s, 1H), 6.44 (d, J = 2.19 Hz, 1H), 5.57−5.55 (m, 1H), 5.23 (s, 2H), 4.66 (d, J = 6.40 Hz, 2H), 3.49 (s, 3H), 1.77 (s, 3H), 1.74 (s, 3H). ^{13}C NMR (125 MHz, $CDCl_3$): δ 177.2, 161.3, 160.4, 160.1, 159.5, 137.4, 131.4, 131.0, 128.8, 125.8, 119.5, 108.9, 98.4, 95.6, 94.3, 66.5, 56.3, 25.7, 18.3. HR-MS (EI): calcd for $C_{22}H_{22}O_5$ $[M]^+$ 366.1467; found, 366.1464.

4.5. Synthesis of Compound 4. Compound **3a** (414 mg, 1.22 mmol) was dissolved in *N,N*-dimethylaniline (15 mL). Then, the solution was heated to 200 °C for 2 h. After the reaction was completed, the resulting mixture was cooled to room temperature and extracted with EtOAc (100 mL × 3) and 1 M HCl (100 mL). The organic layer was dried over $MgSO_4$, filtered, and concentrated under reduced pressure. The crude product was purified by MPLC (EtOAc/Hexane) to give compound **4** (358 mg, 87%).

4.5.1. 6-Allyl-5-hydroxy-7-(methoxymethoxy)-2-phenyl-4H-chromen-4-one (4). ^{1}H NMR (700 MHz, $CDCl_3$): δ 12.87 (s, 1H), 7.87−7.86 (m, 2H), 7.53−7.48 (m, 3H), 6.75 (s, 1H), 6.64 (s, 1H), 6.00−5.95 (m, 1H), 5.29 (s, 2H), 5.04 (dq, J = 17.08, 1.79 Hz, 1H), 4.98 (dq, J = 10.1, 1.6 Hz, 1H), 3.50 (s, 3H), 3.45 (dt, J = 6.19, 1.7 Hz, 2H). ^{13}C NMR (175 MHz, $CDCl_3$): δ 182.6, 163.9, 160.8, 159.0, 156.2, 135.9, 131.8, 131.4, 129.1, 126.3, 114.7, 111.9, 106.2, 105.9, 94.2, 92.6, 56.5, 26.6. HR-MS (EI): calcd for $C_{20}H_{18}O_5$ $[M]^+$ 338.1154; found, 338.1155.

4.6. Synthesis of Compound 5. Compound **4** (300 mg, 0.82 mmol) was dissolved in methanol (7 mL). Then, 1 M HCl (3.28 mL, 3.28 mmol, 4 equiv) was added dropwise to the mixture. The reaction mixture was then stirred at 75 °C for 2 h. After the reaction was completed, the resulting mixture was cooled to room temperature and extracted with EtOAc (50 mL × 2) and deionized water (50 mL). The organic layer was dried over $MgSO_4$, filtered, and concentrated under reduced pressure. The crude product was purified by MPLC (EtOAc/Hexane) to give compound **5** (240 mg, 82%).

4.6.1. 6-Allyl-5,7-dihydroxy-2-phenyl-4H-chromen-4-one (5). ^{1}H NMR (700 MHz, $CDCl_3$): δ 13.10 (s, 1H), 10.96 (s, 1H), 8.08−8.06 (m, 2H), 7.63−7.57 (m, 3H), 6.97 (s, 1H), 6.60 (s, 1H), 4.97 (dq, J = 17.10, 2.07 Hz, 1H), 4.93 (dq, J = 9.92, 2.10 Hz, 1H), 3.29 (dt, J = 6.20 Hz, 1.40, 2H). ^{13}C NMR (175 MHz, DMSO-d_6): δ 181.9, 162.9, 162.2, 158.6, 155.4, 135.7, 131.9, 130.8, 129.1, 126.3, 114.6, 109.3, 105.1, 103.7, 93.3, 26.0. HR-MS (EI): calcd for $C_{18}H_{14}O_4$ $[M]^+$ 294.0892; found, 294.0890.

4.7. Synthesis of Compound 6 and 7. Compound **3b** (400 mg, 1.09 mmol) was dissolved in *N,N*-dimethylaniline (15 mL). Then, the mixture was heated to 230 °C for 3 h. After the reaction was completed, the resulting mixture was cooled to room temperature and extracted with EtOAc (100 mL × 3) and 1 M HCl (100 mL). The organic layer was dried over $MgSO_4$, filtered, and concentrated under reduced pressure. The crude product was purified by MPLC (EtOAc/Hexane) to give compound **6** (112 mg, 28%) and compound **7** (228 mg, 57%).

https://doi.org/10.1021/acsomega.4c07938
ACS Omega 2024, 9, 50491−50503

4.7.1. 5-Hydroxy-7-(methoxymethoxy)-6-(2-methylbut-3-en-2-yl)-2-phenyl-4H-chromen-4-one (6). ^{1}H NMR (700 MHz, $CDCl_3$): δ 13.60 (s, 1H), 7.89−7.87 (m, 2H), 7.55−7.49 (m, 3H), 6.75 (s, 1H), 6.66 (s, 1H), 6.30 (dd, J = 17.42, 10.58 Hz, 1H), 5.21 (s, 2H), 4.88 (dd, J = 17.39, 1.25 Hz, 1H), 4.83 (dd, J = 10.61, 1.30 Hz, 1H), 3.51 (s, 3H), 1.63 (s, 6H). ^{13}C NMR (125 MHz, $CDCl_3$): δ 183.1, 163.5, 162.5, 161.0, 156.1, 150.7, 156.7, 131.9, 131.3, 129.2, 126.4, 118.6, 107.1, 106.4, 105.9, 94.3, 93.4, 56.7, 41.5, 29.2. HR-MS (EI): calcd for $C_{22}H_{22}O_5$ $[M]^+$ 366.1467; found, 366.1466.

4.7.2. 5-Hydroxy-7-(methoxymethoxy)-8-(3-methylbut-2-en-1-yl)-2-phenyl-4H-chromen-4-one (7). ^{1}H NMR (700 MHz, $CDCl_3$): δ 12.69 (s, 1H), 7.88−7.87 (m, 2H), 7.54−7.49 (m, 3H), 6.64 (s, 1H), 6.59 (s, 1H), 5.26 (s, 2H), 5.24−5.21 (m, 1H), 3.55 (d, J = 6.93 Hz, 2H), 3.48 (s, 3H), 1.82 (s, 3H), 1.68 (d, J = 1.05 Hz, 3H). ^{13}C NMR (175 MHz, $CDCl_3$): δ 183.2, 164.1, 160.7, 160.4, 154.7, 132.1, 131.9 (131.92), 131.9 (131.85), 129.3, 122.4, 109.0, 106.1, 105.7, 98.1, 94.4, 56.5, 25.9, 22.2, 18.1. HR-MS (EI): calcd for $C_{22}H_{22}O_5$ $[M]^+$ 366.1467; found, 366.1467.

4.8. Synthesis of Compound 8. Compound **7** (91 mg, 0.25 mmol) was dissolved in methanol (4 mL). Then, 2 M HCl (500 μL, 1 mmol, 4 equiv) was added dropwise to the mixture. The reaction mixture was stirred at 75 °C for 2 h. After the reaction was completed, the resulting mixture was cooled to room temperature and extracted with EtOAc (50 mL × 2) and deionized water (50 mL). The organic layer was dried over $MgSO_4$, filtered, and concentrated under reduced pressure. The crude product was purified by MPLC (EtOAc/Hexane) to give compound **8** (57 mg, 72%).

4.8.1. 5,7-Dihydroxy-8-(3-methylbut-2-en-1-yl)-2-phenyl-4H-chromen-4-one (8). ^{1}H NMR (700 MHz, DMSO-d_6): δ 12.76 (s, 1H), 10.84 (s, 1H), 8.05−8.03 (m, 2H), 7.61−7.57 (m, 3H), 6.95 (s, 1H), 6.31 (s, 1H), 5.21−5.19 (m, 1H), 3.45 (d, J = 6.84 Hz, 1H), 1.76 (s, 1H), 1.63 (s, 1H). ^{13}C NMR (175 MHz, DMSO-d_6): δ 182.1, 163.0, 161.9, 159.1, 154.6, 131.9, 131.04, 131.0, 129.1, 126.2, 122.4, 106.2, 104.9, 103.9, 98.5, 25.4, 21.3, 17.8. HR-MS (EI): calcd for $C_{20}H_{18}O_4$ $[M]^+$ 322.1205; found, 322.1207.

4.9. Synthesis of Compound 9. Chrysin (254 mg, 1 mmol) in DMF (20 mL), was added K_2CO_3 (552 mg, 4 mmol, 4 equiv). Then, allyl bromide (270 μL, 3 mmol, 3 equiv) was added dropwise to the mixture. The reaction mixture was then stirred at room temperature for 18 h. After the reaction was completed, the resulting mixture was extracted with EtOAc (100 mL × 2) and deionized water (100 mL). The organic layer was dried over $MgSO_4$, filtered, and concentrated under reduced pressure. The crude product was purified by MPLC (EtOAc/Hexane) to give compound **9** (282 mg, 84%).

4.9.1. 5,7-Bis(allyloxy)-2-phenyl-4H-chromen-4-one (9). ^{1}H NMR (500 MHz, $CDCl_3$): δ 7.78−7.76 (m, 2H), 7.43−7.39 (m, 3H), 6.57 (s, 1H), 6.48 (d, J = 2.28 Hz, 1H), 6.32 (d, J = 2.28 Hz, 1H), 6.09−5.99 (m, 2H), 5.66 (dq, J = 17.20, 1.61 Hz, 1H), 5.41 (dq, J = 17.28, 1.42 Hz, 1H), 5.31−5.29 (m, 2H), 4.60 (dt, J = 4.65, 1.62 Hz, 2H), 4.55 (dt, J = 5.32, 1.41 Hz, 2H). ^{13}C NMR (175 MHz, $CDCl_3$): δ 176.9, 162.5, 159.5, 159.4, 132.1, 132.0, 131.2, 130.9, 128.7, 125.6, 118.2, 117.5, 109.4, 108.7, 97.7, 93.7, 69.5, 69.0. HR-MS (EI): calcd for $C_{21}H_{18}O_4$ $[M]^+$ 334.1205; found, 334.1206.

4.10. Synthesis of Compound 10. Compound **9** (708 mg, 2.12 mmol) was dissolved in *N,N*-dimethylaniline (20 mL). Then, the mixture was heated to 200 °C for 2 h. After the reaction was completed, the resulting mixture was cooled to room temperature and extracted with EtOAc (100 mL × 3) and 1 M HCl (100 mL). The organic layer was dried over $MgSO_4$, filtered, and concentrated under reduced pressure. The crude product was purified by MPLC (EtOAc/Hexane) to give compound **10** (527 mg, 74%).

4.10.1. 6,8-Diallyl-5,7-dihydroxy-2-phenyl-4H-chromen-4-one (10). ^{1}H NMR (700 MHz, $CDCl_3$): δ 13.10 (s, 1H), 7.89−7.87 (m, 2H), 7.57−7.51 (m, 3H), 6.69 (s, 1H), 6.07−6.06 (m, 1H), 6.05−5.99 (m, 2H), 5.25−5.12 (m, 4H), 3.66 (dt, J = 6.05, 1.50 Hz, 2H), 3.54 (dt, J = 6.22, 1.45 Hz, 2H). ^{13}C NMR (175 MHz, $CDCl_3$): δ 183.1, 163.8, 159.6, 157.9, 153.7, 135.9, 135.7, 131.9, 131.8, 129.3, 126.4, 116.7, 116.1, 108.6, 105.7, 105.5, 14.1, 27.3, 27.0. HR-MS (EI): calcd for $C_{21}H_{18}O_4$ $[M]^+$ 334.1205; found, 334.1208.

4.11. Synthesis of Compound 11. Compound **4** (240 mg, 0.7 mmol) was dissolved in THF-H_2O (10 mL, 9:1). Then, osmium tetroxide (16 mg, 0.07 mmol, 0.1 equiv) and 4-methylmorpholine *N*-oxide (165 mg, 1.4 mmol, 2 equiv) were added to the solution. The resulting solution was stirred at room temperature for 1 h, and then the reaction was quenched by adding saturated aqueous sodium bisulfite at 0 °C. The resulting mixture was extracted with EtOAc (100 mL × 2) and deionized water (100 mL). The organic layer was dried over $MgSO_4$, filtered, and concentrated under reduced pressure. The crude diol was dissolved in methanol-H_2O (10 mL, 2:1). Then, sodium periodate (180 mg, 0.84 mmol, 1.2 equiv) was added to the mixture. The reaction mixture was then stirred at room temperature for 1 h. After the reaction was completed, the resulting mixture was extracted with EtOAc (100 mL × 2) and deionized water (100 mL). The organic layer was dried over $MgSO_4$, filtered, and concentrated under reduced pressure. The crude aldehyde was dissolved in dichloromethane (5 mL) and sodium borohydride (51 mg, 1.4 mmol, 2 equiv) suspended in MeOH was then added to the solution at 0 °C. The resulting mixture was stirred at room temperature for 30 min. After the reaction was completed, the solution was diluted with water (50 mL). The crude product was extracted with EtOAc (50 mL × 2). The organic layer was dried over $MgSO_4$, filtered, and concentrated under reduced pressure. The crude product was purified by MPLC (EtOAc/Hexane) to give compound **11** (84 mg, 35% over 3 steps).

4.11.1. 5-Hydroxy-6-(2-hydroxyethyl)-7-(methoxymethoxy)-2-phenyl-4H-chromen-4-one (11). ^{1}H NMR (700 MHz, $CDCl_3$): δ 13.01 (s, 1H), 7.91−7.89 (m, 2H), 7.56−7.51 (m, 3H), 6.81 (s, 1H), 6.69 (s, 1H), 5.31 (s, 2H), 3.85 (t, J = 6.50 Hz, 2H), 3.52 (s, 3H), 3.04 (t, J = 6.57 Hz, 2H), 1.75 (s, 1H). ^{13}C NMR (175 MHz, $CDCl_3$): δ 182.6, 164.1, 161.2, 159.5, 156.2, 131.9, 131.3, 129.2, 126.4, 110.9, 106.1, 105.9, 94.4, 92.8, 62.3, 56.6, 26.2. HR-MS (EI): calcd for $C_{19}H_{18}O_6$ $[M]^+$ 342.1103; found, 342.1100.

4.12. Synthesis of Compound 12. Compound **7** (216 mg, 0.6 mmol) was dissolved in THF-H_2O (10 mL, 9:1). Then, osmium tetroxide (14 mg, 0.06 mmol, 0.1 equiv) and 4-methylmorpholine *N*-oxide (150 mg, 1.2 mmol, 2 equiv) were added to the solution. The resulting solution was stirred at room temperature for 1 h, and then the reaction was quenched by adding saturated aqueous sodium bisulfite at 0 °C. The resulting mixture was extracted with EtOAc (100 mL × 2) and deionized water (100 mL). The organic layer was dried over $MgSO_4$, filtered, and concentrated under reduced pressure. The crude diol was dissolved in methanol-H_2O (10 mL, 2:1). Then, sodium periodate (154 mg, 0.72 mmol, 1.2 equiv) was added to the mixture. The reaction mixture was then stirred at room

https://doi.org/10.1021/acsomega.4c07938
ACS Omega 2024, 9, 50491−50503

temperature for 1 h. After the reaction was completed, the resulting mixture was extracted with EtOAc (100 mL × 2) and deionized water (100 mL). The organic layer was dried over $MgSO_4$, filtered, and concentrated under reduced pressure. The crude aldehyde was dissolved in dichloromethane (5 mL) and sodium borohydride (45 mg, 1.2 mmol, 2 equiv) suspended in MeOH was then added to the solution at 0 °C. The resulting mixture was stirred at room temperature for 30 min. After the reaction was completed, the solution was diluted with water (50 mL). The crude product was extracted with EtOAc (50 mL × 2). The organic layer was dried over $MgSO_4$, filtered, and concentrated under reduced pressure. The crude product was purified by MPLC (EtOAc/Hexane) to give compound **12** (78 mg, 38% over 3 steps).

4.12.1. 5-Hydroxy-8-(2-hydroxyethyl)-7-(methoxymethoxy)-2-phenyl-4H-chromen-4-one (12). ^{1}H NMR (700 MHz, $CDCl_3$): δ 12.70 (s, 1H), 7.89−7.88 (m, 2H), 7.56−7.51 (m, 3H), 6.65 (s, 1H), 6.63 (s, 1H), 5.28 (s, 2H), 3.90 (t, J = 6.79 Hz, 2H), 3.50 (s, 3H), 3.18 (t, J = 6.82 Hz, 2H), 1.70 (s, 1H). ^{13}C NMR (175 MHz, $CDCl_3$): δ 183.0, 164.1, 161.3, 160,9, 155.3, 106.1, 105.7, 105.5, 98.2, 94.6, 62.3, 56.7, 26.7. HR-MS (EI): calcd for $C_{19}H_{18}O_6$ $[M]^+$ 342.1103; found, 342.1105.

4.13. Synthesis of Compound 1a. Compound **11** (60 mg, 0.18 mmol) was dissolved in methanol (4 mL). Then, 1 M HCl (720 μL, 0.72 mmol, 4 equiv) was added dropwise to the mixture. The mixture was stirred at 75 °C for 2 h. After the reaction was completed, the resulting mixture was cooled to room temperature and extracted with EtOAc (50 mL × 2) and deionized water (50 mL). The organic layer was dried over $MgSO_4$, filtered, and concentrated under reduced pressure. The crude product was purified by MPLC (EtOAc/Hexane) to give compound **1a** (34 mg, 63%).

4.13.1. 5,7-Dihydroxy-6-(2-hydroxyethyl)-2-phenyl-4H-chromen-4-one (1a). ^{1}H NMR (700 MHz, DMSO-d_6): δ 13.11 (s, 1H), 10.92 (s, 1H), 8.08−8.06 (m, 2H), 7.63−7.56 (m, 3H), 6.93 (s, 1H), 6.56 (s, 1H), 4.69 (s, 1H), 3.48 (t, J = 7.80 Hz, 2H), 2.76 (t, J = 7.56 Hz, 2H). ^{13}C NMR (175 MHz, DMSO-d_6): δ 181.9, 162.9, 162.7, 159.0, 155.4, 131.9, 130.8, 129.1, 126.3, 108.5, 105.1, 103.7, 93.4, 59.4, 26.1. HR-MS (EI): calcd for $C_{17}H_{14}O_5$ $[M]^+$ 298.0841; found, 298.0843.

4.14. Synthesis of Compound 1b. Compound **12** (78 mg, 0.23 mmol) was suspended in methanol (4 mL). Then, 2 M HCl (460 μL, 0.92 mmol, 4 equiv) was added dropwise to the mixture. The mixture was stirred at 75 °C for 12 h. After the reaction was completed, the resulting mixture was cooled to room temperature and extracted with EtOAc (50 mL × 2) and deionized water (50 mL). The organic layer was dried over $MgSO_4$, filtered, and concentrated under reduced pressure. The crude product was purified by MPLC (EtOAc/Hexane) to give compound **1b** (48 mg, 70%).

4.14.1. 5,7-Dihydroxy-8-(2-hydroxyethyl)-2-phenyl-4H-chromen-4-one (1b). ^{1}H NMR (700 MHz, DMSO-d_6): δ 12.81 (s, 1H), 10.80 (bs, 1H), 8.10−8.09 (m, 2H), 7.63−7.59 (m, 3H), 6.97 (s, 1H), 6.31 (s, 1H), 4.82 (bs, 1H), 3.57 (t, J = 7.51 Hz, 2H), 2.95 (t, J = 7.39 Hz, 2H). ^{13}C NMR (125 MHz, DMSO-d_6): δ 182.3, 163.1, 162.4, 159.3, 155.2, 132.0, 131.1, 129.2, 126.4, 104.8, 103.9(103.91), 103.9(103.89), 98.5, 60.0, 26.5. HR-MS (EI): calcd for $C_{17}H_{14}O_5$ $[M]^+$ 298.0841; found, 298.0843.

Characterization data (^{1}H NMR, ^{13}C NMR, and mass analysis) for compounds (1−12) were provided in Supporting Information (Figures S1−14).

4.15. Cell Culture and Cell Viability Assay. Macrophage RAW264.7 murine cells (cell line TIB-71) were purchased from the American Type Culture Collection (Manassas, VA, USA). The RAW264.7 cells were cultured in high-glucose Dulbecco's modified Eagle's medium (DMEM; WelGene, Daegu, Korea) containing 10% fetal bovine serum (Gibco BRL, Grand Island, NY, USA) and 100 U/mL penicillin/streptomycin (Invitrogen, Carlsbad, CA, USA) at 37 °C in a humidified atmosphere with 5% CO_2. WST-1 assay was performed to evaluate cell cytotoxicity using an EZ-Cytox cell viability assay kit (DAEIL Lab, Seoul, Korea), using a previously reported method with slight modifications.[40] The RAW264.7 cells were seeded in a 96-well plate (5 × 10^3 cells/well) for 4 h and then treated with synthetic chrysin derivatives dissolved in 0.1% dimethyl sulfoxide (DMSO)/DMEM (2.5, 5, and 10 μM), with or without LPS cotreatment (200 ng/mL; Invitrogen). The cells treated with 0.1% DMSO in DMEM were used as a control. A blank control consisting of 10 μL of the kit solution and 90 μL of DMEM without cells was also included. Following 18 h incubation, 10 μL of the kit solution was added to each well and further incubated for 2 h at 37 °C with 5% CO_2. The cell viability was determined by measuring the produced formazan using a SpectraMax M3 multidetection microplate reader (Molecular Devices, Sunnyvale, CA, USA) at an absorbance of 450 nm. The cell viability was expressed as a relative value compared to the control.

4.16. Measurement of IL-6, TNF-α, and PGE2 Levels. The levels of IL-6, TNF-α, and PGE2 were determined using a previously reported method with minor modifications.[41] RAW264.7 cells were plated in a 48-well plate (0.5 × 10^5 cells/well) and incubated for 4 h. Following incubation, the cells were treated with various concentrations of synthetic samples (2.5, 5, and 10 μM dissolved in 0.1% DMSO/DMEM) for 18 h, in the present of LPS (200 ng/mL). After 18 h incubation, the culture media were collected for the measurement of IL-6, TNF-α, and PGE2 levels. The levels of IL-6 (#558301) and TNF-α (#558299) were determined using mouse CBA ELISA kits (BD Biosciences, San Jose, CA, USA) and PGE2 (#CSB-E07966m) was determined using a mouse ELISA kits (CUSABIO, Wuhan, China) according to each manufacturer's guidelines.

4.17. Western Blotting. The COX-2 protein levels were determined by Western blotting analysis using a previously described method with minor modifications.[25] RAW264.7 cells were plated in a 6-well plate (1.4 × 10^5 cells/well) and incubated for 4 h. After the incubation, the cells were treated with the synthetic samples (10 μM in 0.1% DMSO/DMEM) for 18 h, in the presence of LPS (200 ng/mL). The cells were harvested, lysed with 250 μL radioimmunoprecipitation assay buffer (#89900, Thermo Fisher, Waltham, MA, USA) containing a protease inhibitor (#5872, Cell Signaling Technology, Danvers, MA, USA), and placed on ice for 15 min. Afterward, the cell lysates were collected and centrifuged (16,000 × g, 20 min, 4 °C), and the protein concentrations of samples were measured using a BCA protein assay kit (A55860, Thermo Fisher). Fifteen μL of the lysate samples (0.5 μg/μL) were separated on a 10% sodium dodecyl sulfate-polyacrylamide gel electrophoresis along with a protein marker (PM2510, SMOBIO Technology, Beijing, China) and subsequently transferred onto a polyvinylidene difluoride membrane (#1620177, Bio-Rad, Hercules, CA, USA). Following blocking with 1 × General-Block buffer (TransLab, Daejeon, Korea) for 1 h, the membranes were incubated overnight at 4 °C with primary antibodies, anti-COX-2 (1:1000 dilution; #12282, Cell Signaling Technology) and β-actin

https://doi.org/10.1021/acsomega.4c07938
ACS Omega 2024, 9, 50491−50503

(1:2000 dilution; #4970, Cell Signaling Technology). After overnight incubation, the membranes were incubated for 1 h at room temperature with horseradish peroxidase (HRP)-conjugated antirabbit secondary antibody (1:5000 dilution; ab6721, Abcam). The membranes were then visualized with ECL Western blotting detection reagents (#1863096 and #1863097, Thermo Fisher) in ChemiDoc Imaging System (Bio-Rad).

4.18. In Vitro COX-2 Inhibition Assay. The inhibitory effects of chrysin, compounds **1a** and **8** on the COX-2 enzyme were assessed using the COX-2 inhibitor screening kit (ab283401), based on a previously described method with minor modifications.[42] The test compounds were dissolved in DMSO and subsequently diluted to the target concentrations (0.1, 1, and 10 μM). Each well of the 96-well plate received 10 μL of the diluted compounds, followed by 80 μL of a master mix solution composed of 76 μL assay butter, 1 μL OxiRed probe, 2 μL COX-2 cofactor, and 1 μL human recombinant COX-2 enzyme. The reaction was initiated by adding 10 μL of arachidonic acid solution to each well. A blank control was prepared by mixing 10 μL of DMSO (without test samples), 80 μL of the master mix solution (without enzyme), and 10 μL of the arachidonic acid solution. Fluorescence intensity was measured using a microplate reader at excitation and emission wavelengths of 535 and 587 nm, respectively, at 25 °C. The percentage inhibition was calculated by comparing the fluorescence intensity of the samples with that of the control. The 50% inhibitory concentration (IC_{50}) values were derived from the concentration-inhibition response curves.

4.19. Preparation of Ligands and Protein Structure. The 2D structures of indomethacin, chrysin, compounds **1a**, and **8** were created using ChemDraw (version 19.1). Their stable conformations were then established by MM2 energy minimization calculations in Chem3D (version 19.1). The crystal structure of mouse COX-2 protein (PDB ID: 4COX) was retrieved from RCSB Protein Data Bank (https://www.rcsb.org). Using PyMOL (version 2.3.4), the structure was refined by removing unnecessary elements such as ligands and water molecules, retaining only chain A with 587 amino acid residues for the docking analysis. The protein's energy minimization was conducted using Swiss-PDB Viewer (version 4.1).

4.20. Computational Molecular Docking Study. Molecular docking of indomethacin, chrysin, compounds **1a**, and **8** against COX-2 enzyme was performed using AutoDock Tools (version 1.5.7).[43] The COX-2 structure was augmented with polar hydrogen atoms and Kollman charges. Gasteiger charges were assigned to the structures of chrysin, compounds **1a**, and **8**, and nonpolar hydrogen atoms were merged. For the docking analysis, the ligand-binding site in COX-2 (Figure S18) was enclosed in a box with the number of grid points in the in x × y × z directions (45 × 45 × 65) and a grid spacing of 0.500 Å. The grid-box center was set at x = 22.488, y = 19.534, and z = 11.098 to encompass the active site of COX-2. The docking calculations were conducted using a Lamarckian genetic algorithm with 50 runs. The other parameters were configured with default values. The optimal conformation with the lowest binding free energy (ΔG_{bind}, kcal/mol) was chosen for postdocking analysis. The 2D and 3D binding interactions between the ligands and COX-2 enzyme were visualized using Discovery Studio 2023 and PyMOL software, respectively. To evaluate the reliability of the docking poses, root-mean-square deviation (RMSD) values were calculated between the initial energy-minimized structures and the docked poses for each ligand using PyMOL. RMSD values below 2 Å were considered to be indicative of stable docking poses.[44]

4.21. Investigation of Druglikeness Properties and In Silico ADMET Prediction. The druglikeness properties of indomethacin, chrysin, compounds **1a**, and **8** were assessed using the Lipinski rule of five criteria[45] through the SwissADME online tool (https://www.swissadme.ch). Lipinski's rule of five assessed druglikeness based on the following parameters: molecular weight, lipophilicity (LogP), number of hydrogen bond acceptors, number of hydrogen donors, number of rotatable bonds, and molar refractivity. Furthermore, the pharmacokinetics profiles of indomethacin, chrysin, compounds **1a**, and **8**, including adsorption, distribution, metabolism, excretion, and toxicity (ADMET) properties, were predicted using the admetSAR online server (https://lmmd.ecust.edu.cn/admetsar1).

4.22. Statistical Analyses. All experiments were repeated a minimum of three times, ensuring consistent data. Results are presented as means ± standard deviation (SD). Significant differences were evaluated using a one-way analysis of variance (ANOVA) followed by Tukey-Kramer's test. A p-value of <0.05 was considered statistically significant. All analyses were carried out using GraphPad Prism (version 8; San Diego, CA, USA).

■ ASSOCIATED CONTENT

Data Availability Statement

All data generated or analyzed during this study are included in this published article.

Supporting Information

The Supporting Information is available free of charge at https://pubs.acs.org/doi/10.1021/acsomega.4c07938.

Mass and ^{1}H and ^{13}C NMR spectra of synthetic compounds (**1**−**14**); effects of indomethacin and piroxicam on LPS-stimulated IL-6 production; uncropped Western blot gel images; IC_{50} curves for COX-2 inhibition; COX-2 binding site; and docking pose of indomethacin at COX-2 (PDF)

■ AUTHOR INFORMATION

Corresponding Authors

Jongho Jeon − *Department of Applied Chemistry, College of Engineering, Kyungpook National University, Daegu 41566, Republic of Korea;* orcid.org/0000-0002-0288-0991; Email: jeonj@knu.ac.kr

Eui-Baek Byun − *Advanced Radiation Technology Institute, Korea Atomic Energy Research Institute, Jeongeup 56212, Republic of Korea;* orcid.org/0000-0002-8612-6602; Email: ebbyun80@kaeri.re.kr

Authors

Yuna Lee − *Advanced Radiation Technology Institute, Korea Atomic Energy Research Institute, Jeongeup 56212, Republic of Korea*

Eun Ji Gu − *Department of Applied Chemistry, College of Engineering, Kyungpook National University, Daegu 41566, Republic of Korea*

Ha-Yeon Song − *Advanced Radiation Technology Institute, Korea Atomic Energy Research Institute, Jeongeup 56212, Republic of Korea*

Bo-Gyeong Yoo − *Advanced Radiation Technology Institute, Korea Atomic Energy Research Institute, Jeongeup 56212, Republic of Korea; Department of Food Science and*

https://doi.org/10.1021/acsomega.4c07938
ACS Omega 2024, 9, 50491−50503

Technology, Kongju National University, Yesan 32439, Republic of Korea

Jung Eun Park − *Department of Applied Chemistry, College of Engineering, Kyungpook National University, Daegu 41566, Republic of Korea*

Complete contact information is available at: https://pubs.acs.org/10.1021/acsomega.4c07938

Author Contributions

Yuna Lee: Writing−original draft, Methodology, Formal analysis. Eun Ji Gu: Methodology, Formal analysis. Ha-Yeon Song: Methodology. Bo-Gyeong Yoo: Methodology. Jung Eun Park: Methodology. Jongho Jeon: Writing−review and editing, Supervision, Project administration, Conceptualization, Funding acquisition. Eui-Baek Byun: Writing−review and editing, Supervision, Project administration, Conceptualization, Funding acquisition

Notes

The authors declare no competing financial interest.

■ ACKNOWLEDGMENTS

This work was supported by the National Research Foundation of Korea (NRF) funded by Ministry of Science and ICT (RS-2022-00164733 and RS-2022-00164734).

■ ABBREVIATIONS

ANOVA, one-way analysis of variance; COX-2, cyclooxygenase-2; DIPEA, *N*,*N*-diisopropylethylamine; DMEM, Dulbecco's modified Eagle's medium; DMF, *N*,*N*-dimethylformamide; DMSO, dimethyl sulfoxide; EtOAc, ethyl acetate; HRP, horseradish peroxidase; IL-6, interleukin-6; LPS, lipopolysaccharide; MPLC, medium-pressure liquid chromatography; MOM, methoxymethyl; PGE2, prostaglandin E2; RMSD, root-mean-square deviation; TNF-α, tumor necrosis factor-alpha; ΔG_{bind}, binding free energy

■ REFERENCES

(1) Maruyama, M.; Rhee, C.; Utsunomiya, T.; Zhang, N.; Ueno, M.; Yao, Z.; Goodman, S. B. Modulation of the inflammatory response and bone healing. *Front. Endocrinol.* **2020**, *11*, 386.

(2) Seibert, K.; Masferrer, J. L. Role of inducible cyclooxygenase (COX-2) in inflammation. *Receptor* **1994**, *4* (1), 17−23.

(3) Harris, S. G.; Padilla, J.; Koumas, L.; Ray, D.; Phipps, R. P. Prostaglandins as modulators of immunity. *Trends in immunology* **2002**, *23* (3), 144−150.

(4) Kawahara, K.; Hohjoh, H.; Inazumi, T.; Tsuchiya, S.; Sugimoto, Y. Prostaglandin E2-induced inflammation: Relevance of prostaglandin E receptors. *Biochimica et Biophysica Acta (BBA)-Molecular and Cell Biology of Lipids* **2015**, *1851* (4), 414−421.

(5) Finetti, F.; Travelli, C.; Ercoli, J.; Colombo, G.; Buoso, E.; Trabalzini, L. Prostaglandin E2 and cancer: insight into tumor progression and immunity. *Biology* **2020**, *9* (12), 434.

(6) Akaogi, J.; Nozaki, T.; Satoh, M.; Yamada, H. Role of PGE2 and EP receptors in the pathogenesis of rheumatoid arthritis and as a novel therapeutic strategy. *Endocrine, Metabolic & Immune Disorders-Drug Targets (Formerly Current Drug Targets-Immune, Endocrine & Metabolic Disorders)* **2006**, *6* (4), 383−394.

(7) Bryson, T. D.; Harding, P. Prostaglandin E2 EP receptors in cardiovascular disease: An update. *Biochemical pharmacology* **2022**, *195*, No. 114858.

(8) Labib, M. B.; Fayez, A. M.; EL-Nahass, E. S.; Awadallah, M.; Halim, P. A. Novel tetrazole-based selective COX-2 inhibitors: Design, synthesis, anti-inflammatory activity, evaluation of PGE2, TNF-α, IL-6 and histopathological study. *Bioorg. Chem.* **2020**, *104*, No. 104308.

(9) Moore, P. A.; Hersh, E. V. Celecoxib and rofecoxib: the role of COX-2 inhibitors in dental practice. *Journal of the American Dental Association* **2001**, *132* (4), 451−456.

(10) Mantry, P.; Shah, A.; Sundaram, U. Celecoxib associated esophagitis: review of gastrointestinal side effects from cox-2 inhibitors. *Journal of clinical gastroenterology* **2003**, *37* (1), 61−63.

(11) Dogné, J.-M.; Hanson, J.; Supuran, C.; Pratico, D. Coxibs and cardiovascular side-effects: from light to shadow. *Current pharmaceutical design* **2006**, *12* (8), 971−975.

(12) Hashizume, M.; Mihara, M. Desirable effect of combination therapy with high molecular weight hyaluronate and NSAIDs on MMP production. *Osteoarthritis and cartilage* **2009**, *17* (11), 1513−1518.

(13) Härtel, C.; Von Puttkamer, J.; Gallner, F.; Strunk, T.; Schultz, C. Dose-dependent immunomodulatory effects of acetylsalicylic acid and indomethacin in human whole blood: potential role of cyclooxygenase-2 inhibition. *Scandinavian journal of immunology* **2004**, *60* (4), 412−420.

(14) Nabil-Adam, A.; Elnosary, M. E.; Ashour, M. L.; Abd El-Moneam, N. M.; Shreadah, M. A. Flavonoids Biosynthesis in Plants as a Defense Mechanism: Role and Function Concerning Pharmacodynamics and Pharmacokinetic Properties. In *Flavonoid Metabolism-Recent Advances and Applications in Crop Breeding*; IntechOpen: 2023.

(15) Che, H.; Lim, H.; Kim, H. P.; Park, H. A chrysin analog exhibited strong inhibitory activities against both PGE2 and NO production. *European journal of medicinal chemistry* **2011**, *46* (9), 4657−4660.

(16) Naz, S.; Imran, M.; Rauf, A.; Orhan, I. E.; Shariati, M. A.; Iahtisham-Ul-Haq; IqraYasmin; Shahbaz, M.; Qaisrani, T. B.; Shah, Z. A.; Plygun, S.; Heydari, M. Chrysin: Pharmacological and therapeutic properties. *Life Sci.* **2019**, *235*, No. 116797.

(17) Rauf, A.; Khan, R.; Raza, M.; Khan, H.; Pervez, S.; De Feo, V.; Maione, F.; Mascolo, N. Suppression of inflammatory response by chrysin, a flavone isolated from Potentilla evestita Th. Wolf. In silico predictive study on its mechanistic effect. *Fitoterapia* **2015**, *103*, 129−135.

(18) Gao, S.; Siddiqui, N.; Etim, I.; Du, T.; Zhang, Y.; Liang, D. Developing nutritional component chrysin as a therapeutic agent: Bioavailability and pharmacokinetics consideration, and ADME mechanisms. *Biomedicine & Pharmacotherapy* **2021**, *142*, No. 112080.

(19) Liu, Y.; Song, X.; He, J.; Zheng, X.; Wu, H. Synthetic derivatives of chrysin and their biological activities. *Medicinal Chemistry Research* **2014**, *23*, 555−563.

(20) An, S.; Ko, H.; Jang, H.; Park, I. G.; Ahn, S.; Hwang, S. Y.; Gong, J.; Oh, S.; Kwak, S. Y.; Lee, Y.; Kim, H.; Noh, M. Prenylated Chrysin Derivatives as Partial PPARγ Agonists with Adiponectin Secretion-Inducing Activity. *ACS Med. Chem. Lett.* **2023**, *14* (4), 425−431.

(21) Cho, H.; Yun, C.-W.; Park, W.-K.; Kong, J.-Y.; Kim, K. S.; Park, Y.; Lee, S.; Kim, B.-K. Modulation of the activity of pro-inflammatory enzymes, COX-2 and iNOS, by chrysin derivatives. *Pharmacol. Res.* **2004**, *49* (1), 37−43.

(22) Dao, T. T.; Oh, J. W.; Chi, Y. S.; Kim, H. P.; Sin, K.-S.; Park, H. Synthesis and PGE 2 inhibitory activity of vinylated and allylated chrysin analogues. *Archives of pharmacal research* **2003**, *26*, 581−584.

(23) Byun, E.-B.; Jang, B.-S.; Byun, E.-H.; Sung, N.-Y. Effect of gamma irradiation on the change of solubility and anti-inflammation activity of chrysin in macrophage cells and LPS-injected endotoxemic mice. *Radiat. Phys. Chem.* **2016**, *127*, 276−285.

(24) Song, H. Y.; Sik Kim, W.; Kim, J. M.; Bak, D. H.; Han, J. M.; Lim, S. T.; Byun, E. B. A hydroxyethyl derivative of chrysin exhibits anti-inflammatory activity in dendritic cells and protective effects against dextran sodium salt-induced colitis in mice. *Int. Immunopharmacol.* **2019**, *77*, No. 105958.

(25) Byun, E.-B.; Song, H.-Y.; Kim, W. S.; Han, J. M.; Seo, H. S.; Park, W. Y.; Kim, K.; Byun, E.-H. Chrysin derivative CM1 and exhibited anti-inflammatory action by upregulating toll-interacting protein expression in lipopolysaccharide-stimulated RAW264. 7 macrophage cells. *Molecules* **2021**, *26* (6), 1532.

(26) Lee, J. H.; Ko, Y. B.; Choi, Y. M.; Kim, J.; Cho, H. D.; Choi, H.; Song, H. Y.; Han, J. M.; Cha, G. H.; Lee, Y. H.; Kim, J. M.; Kim, W. S.; Byun, E. B.; Yuk, J. M. CM1, a chrysin derivative, protects from

endotoxin-induced lethal shock by regulating the excessive activation of inflammatory responses. *Nutrients* **2024**, *16* (5), 641.
(27) Daskiewicz, J.-B.; Bayet, C.; Barron, D. Regioselective syntheses of 6-(1, 1-dimethylallyl)-and 8-(3, 3-dimethylallyl) chrysins. *Tetrahedron* **2002**, *58* (18), 3589−3595.
(28) Comte, G.; Daskiewicz, J.-B.; Bayet, C.; Conseil, G.; Viornery-Vanier, A.; Dumontet, C.; Di Pietro, A.; Barron, D. C-Isoprenylation of flavonoids enhances binding affinity toward P-glycoprotein and modulation of cancer cell chemoresistance. *Journal of medicinal chemistry* **2001**, *44* (5), 763−768.
(29) Hirano, T. IL-6 in inflammation, autoimmunity and cancer. *International immunology* **2021**, *33* (3), 127−148.
(30) Webster, J. D.; Vucic, D. The balance of TNF mediated pathways regulates inflammatory cell death signaling in healthy and diseased tissues. *Frontiers in cell and developmental biology* **2020**, *8*, 365.
(31) Minghetti, L. Cyclooxygenase-2 (COX-2) in inflammatory and degenerative brain diseases. *Journal of Neuropathology & Experimental Neurology* **2004**, *63* (9), 901−910.
(32) Feng, C.; Zhao, M.; Jiang, L.; Hu, Z.; Fan, X.; Jiang, J. Mechanism of modified danggui sini decoction for knee osteoarthritis based on network pharmacology and molecular docking. *J. Evidence-Based Complementary Altern. Med.* **2021**, *2021* (1), No. 6680637.
(33) Shefin, B.; Sreekumar, S.; Biju, C. Identification of lead molecules with anti-hepatitis B activity in Bacopa monnieri (L.) Wettst. and Cassia fistula L. through in silico method. *J. Pharm. Biol. Sci.* **2016**, *11*, 16−21.
(34) Lekmine, S.; Benslama, O.; Kadi, K.; Brik, A.; Djeffali, O.; Ounissi, M.; Slimani, M.; Ola, M. S.; Eldahshan, O. A.; Martín-García, A. I.; Ali, A. Preliminary Investigation of Astragalus arpilobus subsp. hauarensis: LC-MS/MS Chemical Profiling, In Vitro Evaluation of Antioxidant, Anti-Inflammatory Properties, Cytotoxicity, and In Silico Analysis against COX-2. *Antioxidants* **2024**, *13* (6), 654.
(35) Mukai, R. Prenylation enhances the biological activity of dietary flavonoids by altering their bioavailability. *Biosci., Biotechnol., Biochem.* **2018**, *82* (2), 207−215.
(36) Chen, X.; Mukwaya, E.; Wong, M.-S.; Zhang, Y. A systematic review on biological activities of prenylated flavonoids. *Pharmaceutical biology* **2014**, *52* (5), 655−660.
(37) Sychrová, A.; Škovranová, G.; Čulenová, M.; Bittner Fialová, S. Prenylated flavonoids in topical infections and wound healing. *Molecules* **2022**, *27* (14), 4491.
(38) Gundogdu-Hizliates, C.; Alyuruk, H.; Gocmenturk, M.; Ergun, Y.; Cavas, L. Synthesis of new ibuprofen derivatives with their in silico and in vitro cyclooxygenase-2 inhibitions. *Bioorganic chemistry* **2014**, *52*, 8−15.
(39) Yu, T.; Lao, X.; Zheng, H. Influencing COX-2 activity by COX related pathways in inflammation and cancer. *Mini reviews in medicinal chemistry* **2016**, *16* (15), 1230−1243.
(40) Kang, M.; Jeong, C. W.; Ku, J. H.; Kwak, C.; Kim, H. H. Inhibition of autophagy potentiates atorvastatin-induced apoptotic cell death in human bladder cancer cells in vitro. *International journal of molecular sciences* **2014**, *15* (5), 8106−8121.
(41) Byun, E. B.; Sung, N. Y.; Yang, M. S.; Lee, B. S.; Song, D. S.; Park, J. N.; Kim, J. H.; Jang, B. S.; Choi, D. S.; Park, S. H.; Yu, Y. B.; Byun, E. H. Anti-inflammatory effect of gamma-irradiated genistein through inhibition of NF-κB and MAPK signaling pathway in lipopolysaccharide-induced macrophages. *Food Chem. Toxicol.* **2014**, *74*, 255−264.
(42) Karagiannis, T. C.; Ververis, K.; Liang, J. J.; Pitsillou, E.; Kagarakis, E. A.; Yi, D. T.; Xu, V.; Hung, A.; El-Osta, A. Investigation of the Anti-Inflammatory Properties of Bioactive Compounds from Olea europaea: In Silico Evaluation of Cyclooxygenase Enzyme Inhibition and Pharmacokinetic Profiling. *Molecules* **2024**, *29* (15), 3502.
(43) Morris, G. M.; Huey, R.; Lindstrom, W.; Sanner, M. F.; Belew, R. K.; Goodsell, D. S.; Olson, A. J. AutoDock4 and AutoDockTools4: Automated docking with selective receptor flexibility. *Journal of computational chemistry* **2009**, *30* (16), 2785−2791.
(44) Holt, P. A.; Chaires, J. B.; Trent, J. O. Molecular docking of intercalators and groove-binders to nucleic acids using Autodock and Surflex. *J. Chem. Inf. Model.* **2008**, *48* (8), 1602−1615.
(45) Lipinski, C. A.; Lombardo, F.; Dominy, B. W.; Feeney, P. J. Experimental and computational approaches to estimate solubility and permeability in drug discovery and development settings. *Advanced drug delivery reviews* **1997**, *23* (1−3), 3−25.

https://doi.org/10.1021/acsomega.4c07938
ACS Omega 2024, 9, 50491−50503